Acta Cryst. (1967). **22**, 808

Polytype Families in Zinc Sulphide Crystals*

By S. Mardix, E. Alexander, O. Brafman and I. T. Steinberger
Department of Physics, The Hebrew University, Jerusalem, Israel

(*Received* 17 *August* 1966)

The concept of a polytype family is defined. Five new polytypes (8 8), $(9\ 7)_3$, $(12\ 4)_3$, $(7\ 4\ 2\ 3)_3$, $(4\ 3\ 3\ 2\ 2\ 2)_3$ belonging to the family 16*L*–48*R* were identified in one vapour-phase grown crystal. Another five $(18\ 2)_3$, (5 3 3 4 2 3), $(11\ 4\ 3\ 2)_3$, $(5\ 2\ 2\ 3\ 5\ 3)_3$, (5 2 2 3 6 2), found in a second crystal, belong to the 20*L*–60*R* family. Such occurrence of several members of the same family in a zinc sulphide specimen is fairly common. Polytype families are discussed in the framework of a geometrical model of polytypism in zinc sulphide crystals, based on periodically recurring slip.

Introduction

In two previous publications (Brafman, Alexander & Steinberger, 1967 and Mardix, Brafman & Steinberger, 1967) nine new zinc sulphide polytypes were reported. These polytypes were found to have well-ordered structures. Their optical properties are dependent essentially on the percentage of hexagonality α (Brafman & Steinberger, 1966) of the structure. It has been stressed that polytypism in ZnS cannot be understood on the basis of the theory (*e.g.* Krishna & Verma, 1965) which applies to polytypism in SiC and that many more ZnS polytypes have to be identified in order to have an adequate experimental basis for solving the problem.

In the present paper the structure of ten more ZnS polytypes will be described. These ten polytypes were found in two vapour phase grown* crystal specimens, five polytypes in each. It will be shown that polytypes of the same specimen have closely related structures. Evidence will be brought to demonstrate that the occurrence of related polytypes in the same spectrum is a fairly common phenomenon and it is due to a periodic slip at certain close-packed atomic planes (Mardix & Steinberger, 1966).

Identification of the polytypes

The reflected intensities I_{hkl} were computed for all possible Zhdanov sequences of the polytypes, utilizing an IBM 7040 computer. For the computation the equation

$$I_{hkl} \propto (f^2_{\mathrm{Zn}} + f^2_{\mathrm{S}} + 2f_{\mathrm{Zn}} f_{\mathrm{S}} \cos 2\pi lp)(A^2_{\mathrm{Zn}} + B^2_{\mathrm{Zn}}) \times \frac{1+\cos^2 2\theta}{\sin 2\theta} \cdot \frac{\cos\theta}{(\cos^2\varphi - \sin^2\theta)^{\frac{1}{2}}}$$

was used. f_{Zn} and f_{S} are the atomic structure factors of Zn and S; $p=\frac{3}{4}m$; θ is the Bragg angle; φ is the angle between the reflecting plane, for a given θ, and the rotation axis. $A_{\mathrm{Zn}} = \Sigma \cos 2\pi(hx+ky+lz)$ and $B_{\mathrm{Zn}} = \Sigma \sin 2\pi(hx+ky+lz)$.

The polarization and Lorentz correction factors were taken into account in the above computation. No correction was done for the absorption. The calculation of this factor is complicated in our case because of the inconvenient forms of the crystals. It was also impossible to work on small samples of crystals, thus eliminating absorption corrections, because of the polytype transformation induced by breaking off small pieces from the specimen at our disposal.

Qualitatively it is evident that the reflexions near the zero line will suffer only a small reduction in intensity whilst reflexions having larger *l*-values will suffer more pronounced weakening.

The period of a polytype was approximately estimated by measuring the distances of the (10.*l*) spots, and afterwards determined accurately by counting the number of spots within a single period of intensities along the (10.*l*) column (Verma & Krishna, 1966).

Photometric measurement of intensities is very inaccurate because of small spot size (0·1 mm) and the unevenness in blackening due to the crystal shape.

On the other hand, it is easy to compare, with a magnifying glass, the relative intensities and to order them in a descending sequence. This sequence of intensities is then divided arbitrarily into seven groups denoted by: *vvs*; *vs*; *s*; *w*; *vw*; *vvw*; *a* (Tables 1–10).

Table 1. *Comparison of calculated and observed intensities for the* 16*H* (8 8) *polytype* (*region* a *of crystal* 175 *S*14)

l	Calc.	Obs.	Further observed relations between intensities
0	4063	*w*	5 > 6
1	1478	*w*	2 > 0 > 1
2	5873	*w*	
3	3369	*w*	
4	27852	*vs*	
5	143330	*vvs*	
6	112139	*vvs*	
7	6924	*w*	
8	11144	*s*	
9	3832	*w*	

The observed intensities were symmetrical with respect to the zero line (*l* = 0).

---

* Part of a Ph.D. thesis to be submitted by one of the authors (S.M.) to the Senate of the Hebrew University.

* Grown and supplied by 'Yissum' Research Development Company, The Hebrew University, Jerusalem, Israel.

Table 2. *Comparison of calculated and observed intensities for the* 48*R* $(9\ 7)_3$ *polytype* (*region* b *of crystal* 175 *S*14)

l	Calc.	Obs.	*l*	Calc.	Obs.	Further observed relations between intensities
1	1436	*w*	$\bar{2}$	4087	*s*	$\overline{17} > \overline{14}$
4	2698	*s*	$\bar{5}$	225	*vvw*	$\overline{14} \gg \overline{20}$
7	5329	*s*	$\bar{8}$	9214	*vs*	$\overline{29} > \overline{20}$
10	2189	*w*	$\overline{11}$	791	*vw*	$7 > 4$
13	53038	*vvs*	$\overline{14}$	104653	*vvs*	$25 > 22$
16	103114	*vvs*	$\overline{17}$	153797	*vvs*	$10 > 1$
19	56582	*vvs*	$\overline{20}$	17373	*vvs*	
22	2620	*s*	$\overline{23}$	10088	*vs*	
25	8266	*s*	$\overline{26}$	1764	*vw*	
			$\overline{29}$	22727	*vvs*	

Table 3. *Comparison of calculated and observed intensities for the* 48*R* $(12\ 4)_3$ *polytype* (*region* c *of crystal* 175 *S*14)

l	Calc.	Obs.	*l*	Calc.	Obs.
1	2326	*vw*	$\bar{2}$	4789	*w*
4	0	*a*	$\bar{5}$	2961	*w*
7	3854	*w*	$\bar{8}$	0	*a*
10	14950	*s*	$\overline{11}$	10397	*w*
13	27464	*s*	$\overline{14}$	122608	*vs*
16	33670	*vs*	$\overline{17}$	249138	*vvs*
19	29410	*s*	$\overline{20}$	0	*a*
22	17888	*s*	$\overline{23}$	7296	*w*
25	5978	*w*	$\overline{26}$	12047	*w*
			$\overline{29}$	11813	*w*

Table 4. *Comparison of calculated and observed intensities for the* 48*R* $(7\ 4\ 2\ 3)_3$ *polytype* (*region* e *of crystal* 175 *S*14)

l	Calc.	Obs.	*l*	Calc.	Obs.	Further observed relations between intensities
1	3467	*vw*	$\bar{2}$	5012	*vw*	$13 > 22$
4	2698	*vw*	$\bar{5}$	13300	*s*	$\overline{17} > \overline{14}$
7	7833	*w*	$\bar{8}$	9212	*s*	$\overline{20} > \bar{5}$
10	10893	*s*	$\overline{11}$	23173	*vs*	$\bar{2} > 1 \simeq 4$
13	87815	*vvs*	$\overline{14}$	66115	*vvs*	
16	27357	*vs*	$\overline{17}$	137924	*vvs*	
19	27125	*vs*	$\overline{20}$	17373	*s*	
22	65925	*vvs*	$\overline{23}$	7988	*w*	
25	6545	*w*	$\overline{26}$	44006	*vvs*	
28	8154	*w*	$\overline{29}$	10895	*w*	

Table 5. *Comparison of calculated and observed intensities for the* 48*R* $(4\ 3\ 3\ 2\ 2\ 2)_3$ *polytype* (*region* d *of crystal* 175 *S*14)

l	Calc.	Obs.	*l*	Calc.	Obs.	Further observed relations between intensities
1	13561	*w*	$\bar{2}$	5152	*vw*	$\overline{14} > \overline{11}$
4	10069	*w*	$\bar{5}$	5793	*vw*	$10 > 13 \simeq 16$
7	9651	*w*	$\bar{8}$	9214	*vw*	$1 > 4 \simeq 7$
10	39600	*vs*	$\overline{11}$	49947	*vvs*	
13	32595	*vs*	$\overline{14}$	87921	*vvs*	
16	39983	*vs*	$\overline{17}$	40146	*vs*	
19	29000	*s*	$\overline{20}$	4655	*vw*	
22	9984	*vw*	$\overline{23}$	106341	*vvs*	
25	87132	*vvs*	$\overline{26}$	6724	*vw*	
28	2185	*vvw*	$\overline{29}$	11648	*vw*	

Table 6. *Comparison of calculated and observed intensities for the* 60*R* $(18\ 2)_3$ *polytype* (*regions* a *and* b *of crystal* 220 *S*2)

l	Calc.	Obs.	*l*	Calc.	Obs.	Further observed relations between intensities
2	4247	*w*	$\bar{1}$	3017	*w*	$\overline{19} > \overline{22}$
5	5366	*w*	$\bar{4}$	1749	*vw*	$2 > \bar{1}$
8	6329	*w*	$\bar{7}$	601	*vw*	$\overline{13} \simeq \bar{4} > \bar{7}$
11	7113	*w*	$\overline{10}$	0	*a*	
14	7706	*w*	$\overline{13}$	1606	*vw*	
17	8116	*w*	$\overline{16}$	16705	*s*	
20	8373	*w*	$\overline{19}$	497253	*vvs*	
23	8531	*w*	$\overline{22}$	177502	*vvs*	
26	8721	*w*	$\overline{25}$	34568	*vs*	
29	9207	*w*	$\overline{28}$	14712	*s*	
			$\overline{31}$	7832	*w*	
			$\overline{34}$	4703	*w*	

Table 7. *Comparison of calculated and observed intensities for the* 20*L* (5 3 3 4 2 3) *polytype* (*region* c *of crystal* 220 *S*2)

l	Calc.	Obs.	*l*	Calc.	Obs.	Further observed relations between intensities
0	3995	*w*				$\bar{7} > 6$
1	3916	*w*	$\bar{1}$	3366	*w*	$\bar{3} > 2 \simeq \bar{8}$
2	383	*vw*	$\bar{2}$	29304	*s*	
3	33773	*s*	$\bar{3}$	1453	*vw*	
4	36113	*s*	$\bar{4}$	77170	*vs*	
5	34080	*s*	$\bar{5}$	2446	*w*	
6	161245	*vvs*	$\bar{6}$	75457	*vs*	
7	33007	*s*	$\bar{7}$	187652	*vvs*	
8	38308	*s*	$\bar{8}$	501	*vw*	
9	96990	*vs*	$\bar{9}$	42862	*s*	
10	47631	*s*	$\overline{10}$	47631	*s*	
11	26609	*w*	$\overline{11}$	60213	*s*	
12	206	*a*	$\overline{12}$	15682	*vw*	

Table 8. *Comparison of calculated and observed intensities for the* 60*R* (11 4 3 2)$_3$ *polytype* (*region* d *of crystal* 220 *S*2)

l	Calc.	Obs.	l	Calc.	Obs.	Further observed relations between intensities
1	1329	*vw*	$\bar{2}$	5092	*w*	$\overline{20} > \overline{17} > \overline{23}$
4	6921	*w*	$\bar{5}$	10013	*s*	$\overline{29} > \overline{26}$
7	5520	*w*	$\bar{8}$	1094	*vw*	$10 > 13$
10	27488	*vs*	$\overline{11}$	206	*vvw*	$19 \simeq 22 > 28 \simeq 31$
13	17252	*vs*	$\overline{14}$	26917	*vs*	
16	11054	*s*	$\overline{17}$	157074	*vvs*	
19	67858	*vs*	$\overline{20}$	203046	*vvs*	
22	51204	*vs*	$\overline{23}$	122221	*vvs*	
25	4631	*w*	$\overline{26}$	17612	*vs*	
28	32500	*vs*	$\overline{29}$	34961	*vs*	
31	29741	*vs*				
34	9499	*w*				

Table 9. *Comparison of calculated and observed intensities for the* 60*R* (5 2 2 3 5 3)$_3$ *polytype* (*region* e *of crystal* 220 *S*2)

l	Calc.	Obs.	l	Calc.	Obs.
2	11098	*w*	$\bar{1}$	3262	*vw*
5	2683	*vw*	$\bar{4}$	12761	*w*
8	12429	*w*	$\bar{7}$	7450	*vw*
11	37539	*s*	$\overline{10}$	9163	*vw*
14	5737	*vw*	$\overline{13}$	60946	*vs*
17	116725	*vvs*	$\overline{16}$	11785	*vw*
20	2093	*vvw*	$\overline{19}$	212292	*vvs*
23	11619	*vw*	$\overline{22}$	64253	*vs*
26	89954	*vs*	$\overline{25}$	17284	*w*
29	10542	*vw*	$\overline{28}$	88804	*vs*
			$\overline{31}$	8968	*vw*

Table 10. *Comparison of calculated and observed intensities for the* 20*L* (5 2 2 3 6 2) *polytype* (*region* f *of crystal* 220 *S*2)

l	Calc.	Obs.	l	Calc.	Obs.	Further observed relations between intensities
0	15978	*w*				$\bar{6} > 9 \simeq \bar{8} \simeq \bar{9}$
1	6078	*vw*	$\bar{1}$	6078	*vw*	$11 > 12$
2	22043	*w*	$\bar{2}$	10996	*w*	$2 > 0 \simeq \bar{7}$
3	6861	*vw*	$\bar{3}$	6861	*vw*	$\bar{7} > \bar{4} > \bar{2}$
4	29476	*s*	$\bar{4}$	13794	*w*	
5	54791	*vs*	$\bar{5}$	54791	*vs*	
6	61204	*vs*	$\bar{6}$	285799	*vvs*	
7	16727	*w*	$\bar{7}$	16727	*w*	
8	1313	*vvw*	$\bar{8}$	100291	*vvs*	
9	97774	*vvs*	$\bar{9}$	94774	*vvs*	
10	14656	*vw*	$\overline{10}$	14656	*w*	
11	58837	*s*	$\overline{11}$	58837	*s*	
12	41057	*s*	$\overline{12}$	537	*a*	

The identification of the polytype is effected by looking amongst the calculated intensities for the sequence that fits the observed data.

This procedure leads to a unique identification of the polytype even if the relative intensities of only a small number (about five) of reflexions are used.

As an example we shall bring the identification procedure of the 20*L* (5 2 2 3 6 2) polytype.

An X-ray photograph of the (10.*l*) column is given in Fig. 3 and the intensity data in Table 10.

From the X-ray photograph it is seen that the 8th spot above the zero line is the weakest, whilst the 6th spot below the equator is the strongest one.

From birefringence measurements it was concluded (Brafman, Alexander & Steinberger, 1966) that the number of Zhdanov numbers in the sequence of this 20*L* polytype is six.

The overall number of such sequences is about 680. Only 40 of them have a weak spot belonging to $l = +8$ or $l = -8$ (not necessarily the weakest); 14 of these sequences have a very strong spot for $l = -6$ (or $l = +6$). The further observation that spots nos. -8 and -9 (below the equator) are stronger than nos. -9 and -10, leaves us with only one fitting sequence, namely (5 2 2 3 6 2). The fit of the other reflexion intensities in the same column, which have not been mentioned above, fully confirms the identification.

Had the comparison been started with a different set of spots, this procedure would have led to the same identification.

It is pointed out that this identification procedure is based on the fact that large variations occur in the intensity distributions calculated for the various Zhdanov sequences. Therefore any occasional small discrepancy found between the calculated intensities of the 'fitting' sequence and the observed intensities of a certain spot (which may be due to the neglected absorption correction) is immaterial for identification purposes.

Results

Black and white photomicrographs of the crystals, as seen between partially crossed polarizers, are presented in Figs. 1(*a*) and 2(*a*). Direct observation reveals, in each crystal, a set of parallel colored bands due to variations of birefringence (see, *e.g.* Brafman & Steinberger, 1966). The faces of crystal regions differing in birefringence are usually tilted with respect to each other. It should be emphasized that in spite of the tilts the direction of the *c* axis stays constant throughout each specimen, as indicated by the arrows. Fine striations appear in the figures; they are parallel to each other and perpendicular to the common *c* axis.

Some crystal regions between neighboring striations are indicated and named in the Figures. Each region of this kind has a uniform birefringence. Particularly interesting adjacent regions are represented, with a higher magnification, in Figs. 1(*b*) and 2(*b*). The birefringence of the neighbors is the same in these cases, but a fine striation appears between them and a slight angle of tilt can also be perceived.

X-ray oscillation photographs around the *c* axis were taken within the crystal regions named in Figs. 1(*a*) and 2(*a*). All the X-ray photographs showed well-defined and sharp reflexion spots, with no appreciable

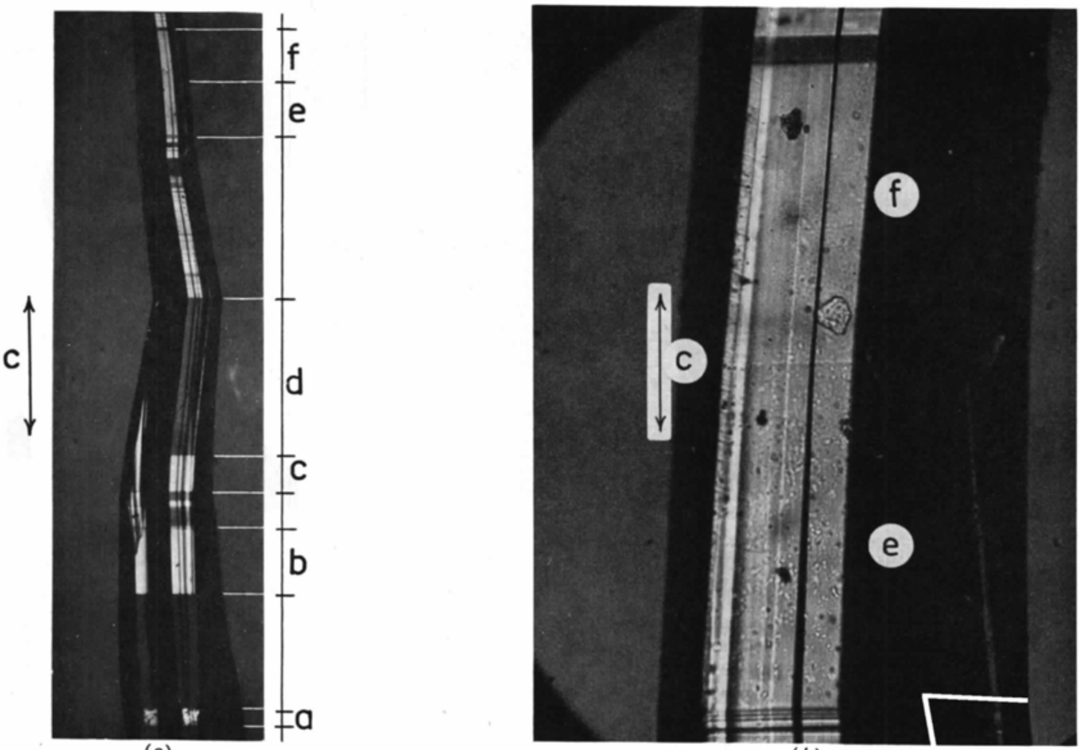

(*a*) (*b*)

Fig. 2.(*a*) Black and white photograph of crystal 220 *S*2 between nearly crossed polarizers (× 24). (*b*) Regions *e* and *f* of Fig. 2(*a*) (× 150).

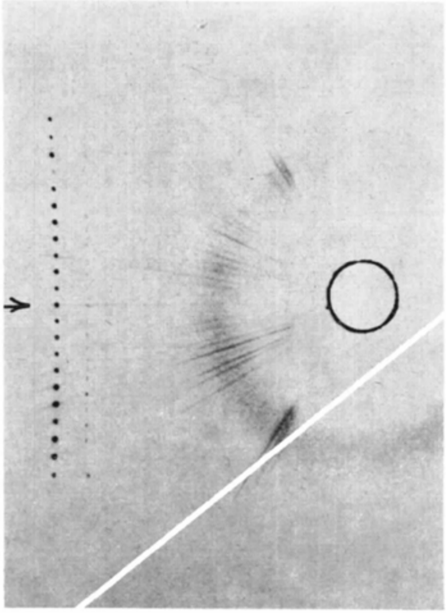

Fig. 3. (10.*l*) column of an oscillation photograph around the *c* axis of the 20*L* (5 2 2 3 6 2) polytype. Cu $K\alpha$ radiation, 60 mm dia. camera (× 3). The position of the zero line is indicated by an arrow.

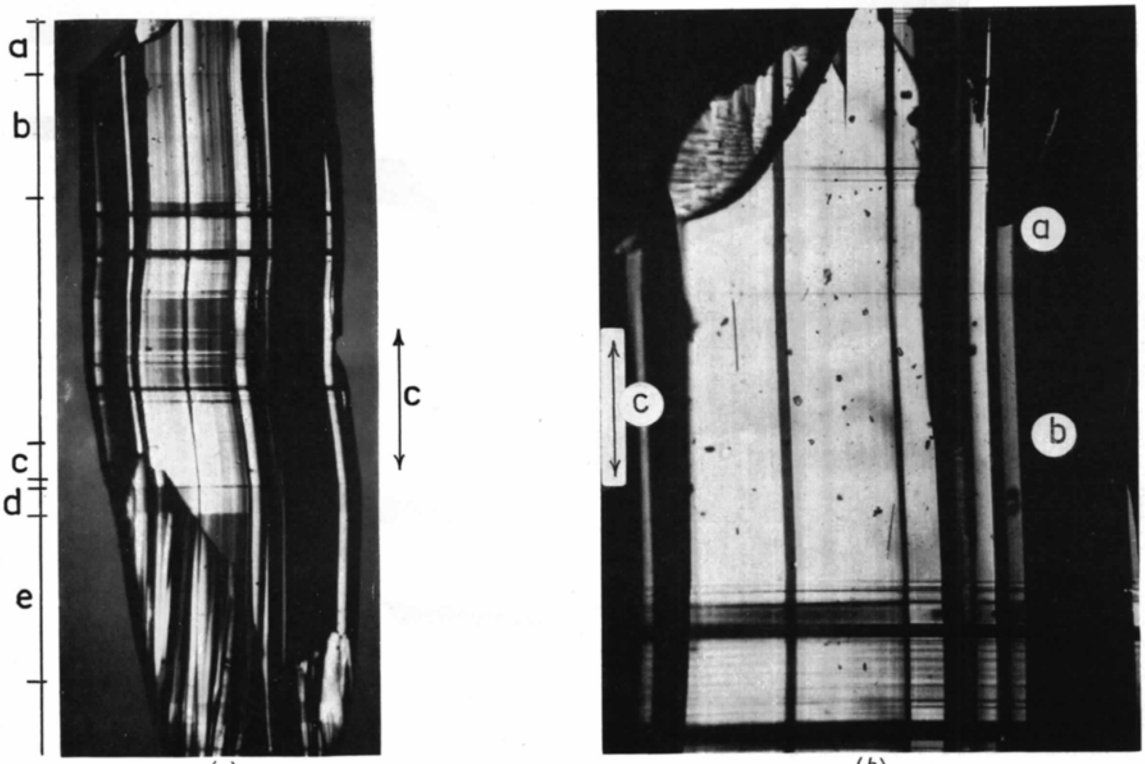

(a) (b)

Fig. 1.(*a*) Black and white photograph of crystal 175 *S*14 between nearly crossed polarizers (× 24). (*b*) Regions *a* and *b* of Fig. 1(*a*) (× 57).

'smearing out'. It follows that the structure of the regions named in Figs. 1(*a*) and 2(*a*) are well-defined and one-dimensional stacking disorder can be neglected.

The observed X-ray reflexion intensity distributions (for the (10.l) columns) and the only fitting calculated ones are given in Tables 1 to 10. The hundreds of other calculated non-fitting distributions belonging to the correct unit-cell dimensions but to the wrong layer sequences are not presented because of lack of space. All structures reported here are new ZnS polytypes; their crystallographic description is summarized in Table 11.

The degree of birefringence of the polytypes, Δn, was found to be proportional to α, in accord with results for other ZnS polytypes (Brafman & Steinberger, 1966; Mardix, Brafman & Steinberger, 1967).

The five identified structures of the crystal 175 *S*14 have either a 16-layer or a rhombohedral 48-layer unit cell; those of the crystal 220 *S*2 have either a 20-layer unit cell or a rhombohedral 60-layer one.

The polytypes in each of the described specimens will be henceforth regarded as being members of the same 'polytype family'; a family is defined here as consisting of all structures with the same periodicity *m*, as well as of the rhombohedral structures with 3*m*-layer periodicity.

Discussion

A prominent result of the present work is the occurrence of several members of the same polytype family in a single specimen. Six other specimens were found each including a different identified polytype family. These polytype families are: 6*H*–18*R*, 8*H*–24*R*, 10*L*–30*R*, 24*L*–72*R*, 32*L*–96*R* and 40*L*–120*R*. Farkas-Jahnke (1965) also reports a ZnS crystal which includes several 24-layer polytypes. The crystals described include, apart from the wide regions mentioned, many narrow regions of unknown structures as well. However, the values of birefringence measured in the wide regions recur in the narrow ones. As the degree of birefringence yields directly the percentage of hexagonality of the structure (Brafman & Steinberger, 1966), it seems likely that most of the narrow bands also belong to the same polytype family. It should be noted in this respect that even crystals consisting solely of a large number of narrow bands exhibit only few well-defined degrees of birefringence, recurring many times.

The occurrence of several members of a polytype family in a single specimen can be understood on the basis of allotropic transformations observed in ZnS crystals (Mardix & Steinberger, 1966). It has been stated that transformations from a given polytype to another one can take place owing to slips by vectors of the type $a/3[21.0]$, recurring periodically at certain (00.1) planes. Such transformations by periodic slips were indicated from correlation between tilt angles and structures (Mardix & Steinberger, 1966). Regions *a* and *b* of crystal 175 *S*14 (Table 11) furnish a simple example of the periodic slip process. Region *a* has the Zhdanov symbol (8 8), *i.e.* in the unit cell eight (00.1) planes are stacked in cyclic order and eight in anticyclic order. Slip by an $a/3[21.0]$ vector at the ninth plane (in each unit cell) transposes this plane to the cyclic part of the period. The structure thus transforms to $(9\ 7)_3$.

Regions *e* and *f* of crystal 220 *S*2 furnish another example of such a transformation. In these cases the change of structure is revealed under the microscope by the tilt (Mardix & Steinberger, 1966) and the striation between the neighboring regions [Figs. 1(*b*) and 2(*b*)]. There is no change in birefringence, since the percentage of hexagonality stays constant in these transformations.

If in an *m*-layer polytype more than one slip per unit cell takes place, and the slips recur with the period of the lattice, other members of the *m*-layer polytype family will be generated (with various percentages of hexagonality). The appearance of several members of the same family in a specimen may thus be simply understood by assuming that most of the crystal has been composed of a single *m*-layer polytype region. Its various parts have subsequently undergone different periodic slips, all being of the type described above and therefore belonging to the same family.

In principle it is possible to generate polytypes from the hexagonal 2*H* structure by slips which recur with a periodicity larger than that of the 2*H* lattice. 'Even polytypes' (those where the sum of the elements of the

Table 11. *Description of new* ZnS *polytypes*

Crystal notation	Region	Polytype	Layer sequence	Per cent hexagonality α	Space group
175 *S*14	*a*	16*H*	(8 8)	12·5	$P6_3mc$
	b	48*R*	$(9\ 7)_3$	12·5	$R3m$
	c	48*R*	$(12\ 4)_3$	12·5	$R3m$
	d	48*R*	$(4\ 3\ 3\ 2\ 2\ 2)_3$	50·0	$R3m$
	e	48*R*	$(7\ 4\ 2\ 3)_3$	25·0	$R3m$
220 *S*2	*a*	60*R*	$(18\ 2)_3$	10·0	$R3m$
	b	60*R*	$(18\ 2)_3$	10·0	$R3m$
	c	20*L*	(5 3 3 4 2 3)	30·0	$P3m1$
	d	60*R*	$(11\ 4\ 3\ 2)_3$	20·0	$R3m$
	e	60*R*	$(5\ 2\ 2\ 3\ 5\ 3)_3$	30·0	$R3m$
	f	20*L*	(5 2 2 3 6 2)	30·0	$P3m1$

Zhdanov sequence is even) as well as the cubic (∞) structure will be generated in this way. The 'parent polytype' could thus be formed from the 2*H* structure.

All the above considerations deal only with the geometrical framework of polytypism in ZnS crystals. Further experiments are in progress in order to ascertain the physical mechanism underlying the slip process.

Actually it seems that all polytypes in vapour-phase grown crystals are even*. In this Laboratory, altogether about 35 polytypes were found, with 21 different layer periodicities, all being even. The literature on polytypes in vapour-phase grown ZnS seems also to confirm this rule, except for a very early publication (Strock & Brophy, 1955) on a single extremely small specimen (0·1 × 0·01 mm) which was reported to include altogether nine structures.

Direct observations in this Laboratory (to be published) revealed that the hexagonal 2*H* structure can actually be transformed to polytypes, and that this transformation takes place by the periodic slip process. The overall route of polytype formation is therefore probably the following: hexagonal – parent polytype – polytype family.

References

BRAFMAN, O., ALEXANDER, E. & STEINBERGER, I. T. (1967). *Acta Cryst.* **22**, 347.

BRAFMAN, O. & STEINBERGER, I. T. (1966). *Phys. Rev.* **143**, 501.

FARKAS-JAHNKE, M. (1965). *Acta Cryst.* **18**, 571.

KRISHNA, P. & VERMA, A. R. (1965). *Z. Kristallogr.* **121**, 36.

MARDIX, S., BRAFMAN, O. & STEINBERGER, I. T. (1967). *Acta Cryst.* **22**, 000.

MARDIX, S. & STEINBERGER, I. T. (1966). *Israel J. Chem.* **3**, 243.

STROCK, W. & BROPHY, V. A. (1955). *Amer. Min.* **40**, 94.

VERMA, A. R. & KRISHNA, P. (1966). *Polymorphism and Polytypism in Crystals.* New York: John Wiley.

---

* Uneven polytypes 9*R*, 15*R* and 21*R* were found in ZnS minerals. A 27*L* polytype reported by two of us (O.B. & I.T.S.) was later found to be a 26*L* (17 4 2 3) polytype.

Acta Cryst. (1967). **22**, 812

Reinvestigation of the Crystal Structure of Ammonium Bromochloroiodate(I), NH$_4$BrICl, at 140° K

BY TINY MIGCHELSEN AND AAFJE VOS

Laboratorium voor Structuurchemie, Rijksuniversiteit Groningen, Bloemsingel 10, *Groningen, The Netherlands*

(*Received* 5 *September* 1966)

Reinvestigation of the crystal structure of NH$_4$BrICl at 140°K shows that the (BrICl)$^-$ ions are statistically distributed in the crystal. Owing to this disorder no accurate values could be obtained for the bond lengths. The discussion of the observed average structure indicates, however, that for (BrICl)$^-$ ions with an orientation as reported earlier by Mooney, the I–Cl bond is much longer (*ca.* 0·5 Å) than the value which Mooney observed (2·38 Å). The I–Br distance is comparable to Mooney's value, 2·50 Å.

Description of the structure

As part of a programme to obtain accurate values for bond lengths and angles in polyhalide ions consisting of different halogen atoms (KICl$_4$.H$_2$O, Elema, de Boer & Vos, 1963; N(CH$_3$)$_4$ICl$_2$, Visser & Vos, 1964), the structure of NH$_4$BrICl (Mooney, 1937) was reinvestigated at 140°K.

The structure as reported by Mooney is shown in Fig. 1. The present refinement shows that accurate values for the bond lengths and angles cannot be obtained because of disorder in the crystals. The discussion given in the present paper indicates, however, that for the (Br–I–Cl)$^-$ ion shown in Fig. 1, the I–Cl bond is much longer, approximately 0·5 Å, than the value observed by Mooney, 2·38 Å, and considerably longer than the sum of the covalent radii, 2·33 Å. The I–Br distance is comparable to Mooney's value, 2·50 Å.

As in the isomorphous compound CsI$_2$Br (Carpenter, 1966) there is one short intermolecular distance, $\mathrm{I}(3)\cdots\mathrm{Br}(1) \simeq 3{\cdot}64$ Å (van der Waals distance 4·10 Å). This distance is observed in a nearly linear I···Br–I–Cl chain (Fig. 1, Table 3), suggesting that the bonding may be described as 4-center, 6-electron bonding (Hach & Rundle, 1951; Pimentel, 1951).

Experimental

Crystals were prepared according to Mooney's method. The halogen composition of the sample found by chemical analysis (I = 46·9, Br = 31·1, Cl = 13·6%) showed reasonable agreement with the formula NH$_4$BrICl (I = 48·7, Br = 30·7, Cl = 13·6%).

The crystallographic data were obtained from Weissenberg photographs taken at 140°K. The crystals are orthorhombic; the systematic absences indicate as pos-